sciendo
ISSN 1335-8871
MEASUREMENT SCIENCE REVIEW
Journal homepage: https://content.sciendo.com

Metamaterial Inspired Stub-Incorporated Quad-Band Diamond Shaped Monopole Antenna for Satellite and Wireless Application

Jansirani G*, Gandhi Raj R

Department of Electrical and Electronics Engineering, University College of Engineering (BIT Campus), Anna University, Tiruchirappalli, Tamil Nadu, India, g.jansirani@rediffmail.com, gandhirajeee@gmail.com

Abstract: This study presents a quad-band stub-incorporated split octagonal ring antenna specifically designed for wireless applications that rely on satellite communication. The antenna is fabricated on an FR4 substrate with dimensions of 26×21×1.6 mm³ and its performance is simulated using the CST EM Studio software. The device operates in the frequency range from 2.15 GHz to 6.35 GHz, using stub integration and gap modification to achieve resonant bands. The antenna has resonant frequencies of 2.23 GHz, 3.28 GHz, 4.77 GHz, and 5.89 GHz, with corresponding bandwidths of 153 MHz, 9011 MHz, 7692 MHz, and 6813 MHz, respectively. The parametric analysis optimizes the values of the design parameters, while the experimental validation shows the consistency between the measured and simulated results. The antenna is characterized by a small size, a consistent radiation pattern and a wide range of applications including ISM, WIFI, WLAN, WIMAX, 5G, and C-Band Satellite. The device is capable of operating in two frequency bands and consistently maintains a gain of over 1 dBi across its resonating range.

Keywords: Quad-band antenna, satellite communication, stub-incorporated design, wireless applications, frequency band optimization.

1. INTRODUCTION

The rise of Satellite Communication-dependent wireless applications has led to a significant demand for multiband antenna solutions. Multiband antennas, which can operate in multiple frequency bands, have become essential in the realm of handheld mobile devices, where compactness is essential due to limited space. As these devices serve numerous applications simultaneously, the need for smaller antennas has intensified. In particular, multiband antennas [1] have attracted the attention of researchers as they have the potential to streamline system designs. By reducing the need for multiple antennas and eliminating the need for complex filters found in multiband systems, they offer notable advantages, including reduced manufacturing, installation and cost burden. In addition, dual-band antennas hold appeal across various fields such as wireless communication, RFID technology and microwave energy production, as they require less space and necessitate fewer antennas [2].

Compact multiband antennas have effectively integrated elements inspired by metamaterials [3]-[5]. As discussed in [6], researchers have explored a range of metamaterials to improve the performance of antennas based on metamaterial principles. In [7], the research focused on improving antenna performance by using metamaterial-inspired designs consisting of one or more unit cells. Metamaterial-inspired antennas have been instrumental in various aspects, including impedance matching, bandwidth increase, gain improvement, compactness, and multiband antenna design, as highlighted in studies [8]. These advances emphasize the potential of metamaterial-inspired approaches to address key challenges in antenna engineering and pave the way for more efficient and versatile antenna designs.

The amalgamation of resonant structures, such as Split Ring Resonators (SRR) and closed ring resonators, led to the development of a dual-band Coplanar Waveguide (CPW)-fed antenna (CRR). In addition, a portable Ultra-Wideband (UWB) antenna was developed using a compact circular disc and a circular spiral ring resonator [9]. The CPW feed was intricately integrated with a quarter-wave transformer to ensure robust impedance matching, due to the small size of the SRR [10]. To enable multiband operation, a microstrip patch resembling a rectangle equipped with Complementary Split Ring Resonators (CSRRs) and fed from the left offset was introduced [11]. It has also been proposed that a CSRR-filled conductor-backed CPW antenna be employed for operation across three bands. Despite the advances, the prevailing antennas in research suffer from limitations such as complex designs, larger footprints and erratic radiation patterns. Consequently, there is a pronounced demand for smaller antennas that offer optimal performance. By carefully placing radiating elements, parasitic elements, or reactive components, the antenna can resonate at different frequencies

DOI: 10.2478/msr-2024-0020

Corresponding author: g.jansirani@rediffmail.com (G.Jansirani)

simultaneously. To maximize the bandwidth around each resonant frequency, fine-tuning the dimensions of the radiating element is necessary.

2. EVOLUTION OF METAMATERIAL RING ANTENNA

The proposed antenna, developed with the CST EM software, consists of a split octagonal ring incorporated into a stub. The development of the antenna can be divided into three stages: Ant A, Ant B, and Ant C. The proposed stub-incorporated octagonal SRR is shown in Fig. 1. Constructed on an FR4 substrate with a dielectric constant of 4.4, the antenna has an overall dimension of 21 mm in width and 26 mm in length. Fig. 2 shows the proposed antenna with its dimensions and other relevant features, while Table 1 presents the parameters and their corresponding values. Ant A is a basic four-sided ring structure with a shallower ground plane that can operate in two different frequency ranges: between 2.43 and 3.25 GHz and between 6.65 and 7.91 GHz. The bandwidth of Ant A varies between 825 and 1269 MHz, depending on the operating band. The seed antenna, Ant A, resonates at frequencies of 2.82 and 7.30 GHz.

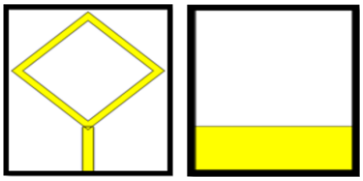

(a) Ant A

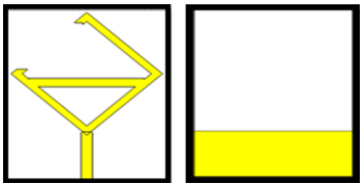

(b) Ant B

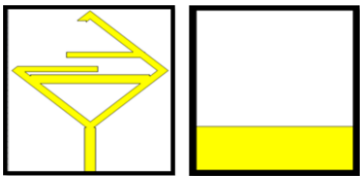

(c) Ant C

Fig. 1. Metamaterial ring antenna – antenna evolution.

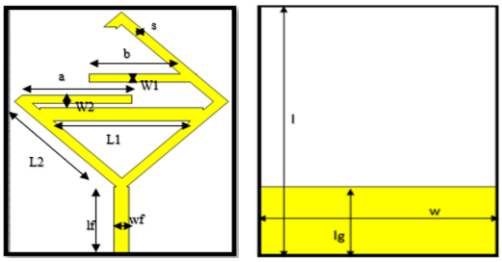

Fig. 2. Metamaterial ring antenna – antenna parameters.

Ant B is formulated by converting the closed ring resonator into a split ring resonator and introducing a stub of length l2 connected across the split ring at its center. This change in structure leads to a change in the current direction, thereby increasing inductance and capacitance. Consequently, the operating frequency bands are reduced. Ant B resonates at 2.37 GHz and 5 GHz, with the operating frequency ranging from 2.21 GHz to 2.53 GHz and from 4.00 GHz to 5.83 GHz. The bandwidth of Ant B is measured at 317 MHz and 1831 MHz, respectively.

In the last stage, Ant C, two more stubs are added, changing the current direction and increasing the electrical length of the antenna. This change leads to additional resonance. The proposed antenna design resonates in four different frequency bands with operating frequencies of 2.15 GHz to 2.30 GHz, 2.86 GHz to 3.76 GHz, 4.47 GHz to 5.24 GHz, and 5.67 GHz to 6.35 GHz, respectively. The resonant frequencies of the antenna are 2.23 GHz, 3.28 GHz, 4.77 GHz, and 5.89 GHz, with corresponding bandwidths of 153 MHz, 9011 MHz, 7692 MHz, and 6813 MHz, respectively. The critical dimensions of the proposed antenna are shown in Fig. 3.

Table 1. Parameter values of metamaterial ring antenna (in mm).

L	w	Lg	lf	wf	l1	l2
26	21	7.6	7.2	1.5	9	15.38
w1	w2	a	b	s	h	t
0.52	0.15	9.01	7.53	1.5	1.6	0.035

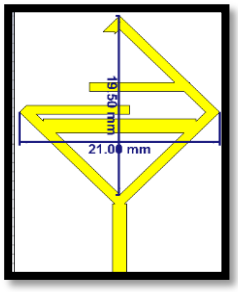

Fig. 3. Metamaterial ring antenna – antenna dimensions.

Fig. 4 shows the return loss plot for all three stages of antenna development, demonstrating that with the introduction of the split and the stub, the proposed antenna resonates at four different bands. Fig. 5 and Fig. 6 show the antenna's return loss S11 and Voltage Standing Wave Ratio (VSWR) as a function of frequency. At 2.23 GHz the antenna has a return loss of -13.52 dB; at 3.28 GHz the return loss is -25.12 dB; at 4.77 GHz it is-34.14 dB; and at 5.89 GHz the return loss is-24.83 dB. In addition, the VSWR values in the resonant bands are all below 2 dB, indicating excellent impedance matching of the proposed structure.

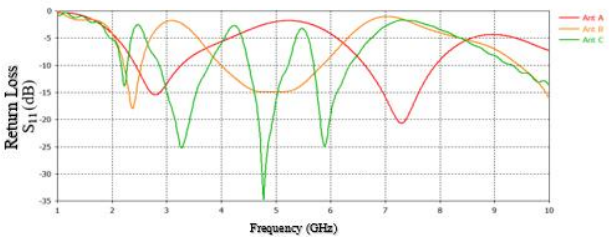

Fig. 4. S11 Comparison of the metamaterial ring antenna.

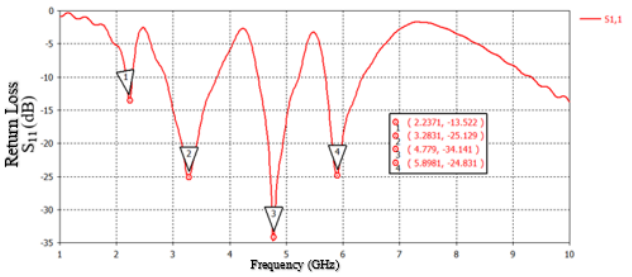

Fig. 5. S11 – Ant C.

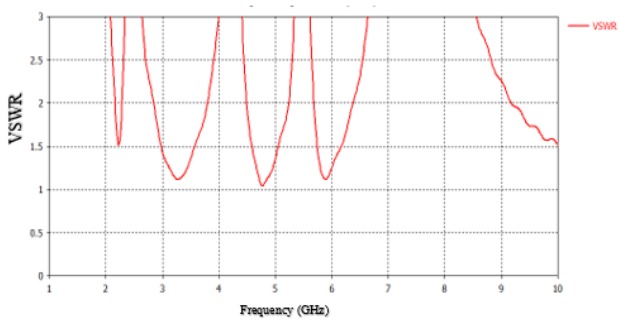

Fig. 6. VSWR – Ant C.

3. PARAMETRIC ANALYSIS

The performance of the antenna is in fact highly dependent on the dimensions of the critical parameters. Achieving optimal performance requires a meticulous analysis of these dimensions. Parametric analysis is a valuable tool to systematically investigate how the variations of the parameters affect antenna performance. By systematically varying key parameters within defined ranges, parametric analysis enables the identification of optimal dimensions that maximize desired performance metrics such as bandwidth, return loss and radiation pattern characteristics. This iterative process enables antenna designers to fine-tune critical dimensions to achieve desired performance goals. Parametric analysis allows designers to explore a wide range of parameter combinations to fully understand their impact on antenna performance. This approach facilitates the optimization of antenna design and ensures that critical parameters are carefully tuned to achieve the best possible performance under different operating conditions and requirements.

Fig. 7 shows the return loss performance for different numbers of stubs, demonstrating that the inclusion of stubs leads to an increase in the number of operating bands. Specifically, the split octagonal antenna with a single stub has three operating frequencies, while the addition of an extra stub transforms the antenna into a quad-band system. Thus, the stub is credited with enabling the additional resonant band. Specifically, the single stub-split octagonal ring antenna operates at frequencies of 2.3 GHz, 2.9 GHz and 5.1 GHz. Following the introduction of a second stub, the antenna operates at 2.23 GHz, 3.28 GHz, 4.77 GHz and 5.89 GHz, demonstrating its ability to operate over a wider frequency range. This highlights the significant role played by stubs in extending the operating bandwidth of the antenna system, improving its versatility and performance.

In the subsequent phase, incremental adjustments are made to the ground length and the resulting effects are analyzed, as shown in Fig. 8. It can be seen that the impedance matching in each of the resonant bands is satisfactory when the ground length is set to 7.8 mm. Therefore, this value is chosen as the optimal ground length for further calculations. In addition, the width of the outer ring is investigated, with the ring width varying from 1 mm to 2 mm in increments of 0.5 mm throughout the study. Fig. 9 illustrates the effect of the ring width on the return loss plot. It can be seen that a ring width of 1.5 mm yields good impedance-matching bandwidth across all resonant bands. Therefore, this value is considered suitable for the manufacturing process, serving as the final chosen value.

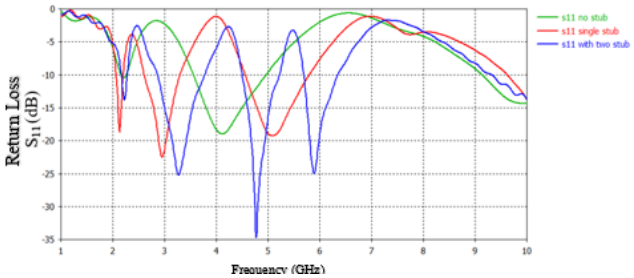

Fig. 7. Parametric analysis – stub effect.

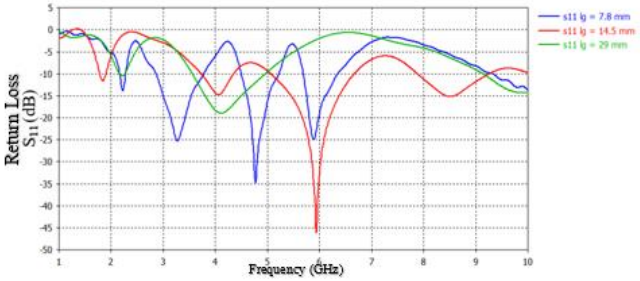

Fig. 8. Parametric analysis – length of ground.

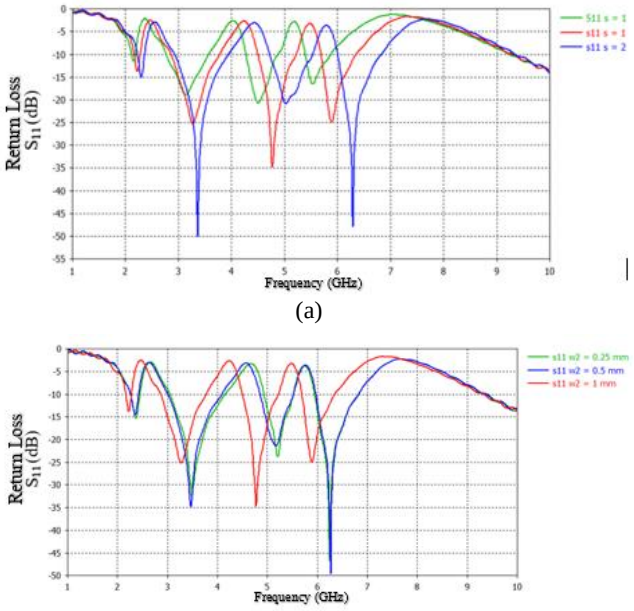

Fig. 9. Parametric analysis: (a) width of rings, (b) stub distance.

The effect of the distance between the stubs is shown in Fig. 10. Starting from 0.25 mm and in steps of 0.25 mm up to 1 mm, the distance between the stubs is systematically varied. The evaluation shows that the impedance matching is significantly improved if the distance between the stubs is set to 1 mm across all resonant bands. Therefore, this distance value is adopted for the final fabrication to ensure optimal performance over the antenna's operating frequency range.

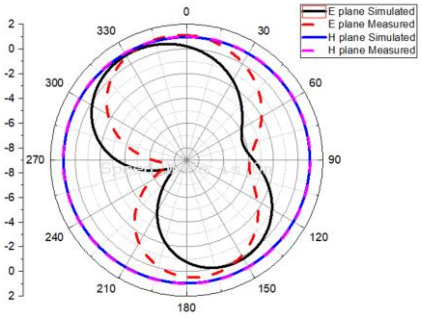

(a) 2.4 GHz

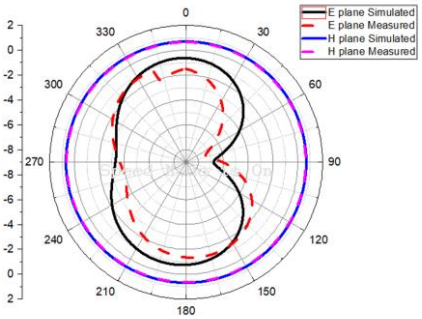

(b) 3.2 GHz

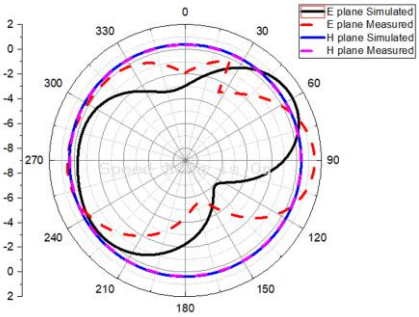

(c) 4.7 GHz

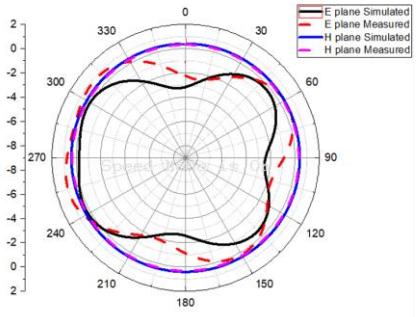

(d) 5.9 GHz

Fig. 10. Metamaterial ring antenna – E plane and H plane at various resonating band.

4. RESULTS AND DISCUSSION

At a frequency of 2.4 GHz, the surface current peaks throughout the proposed structure. Near stub one, the surface current peaks at 3.2 GHz, while near stub two it peaks at 4.7 GHz, indicating that the antenna is responsible for the 4.7 GHz band. At 5.9 GHz, the maximum surface current is observed between the gaps of the stub. The surface current distribution shown in Fig. 11 indicates that the introduction of stubs changes the current direction, leading to the emergence of new resonant bands.

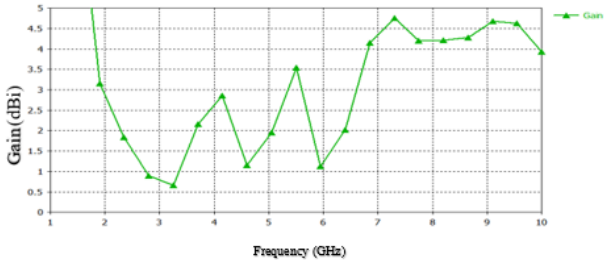

Fig. 11. Metamaterial ring antenna – gain vs. frequency.

The radiation patterns for the E-plane and the H-plane are shown in Fig. 10, which depicts a split octagonal antenna. The figure clearly shows that the radiation pattern of the E-plane is that of an eight-shaped dipole, while the radiation pattern of the H-plane is an omnidirectional pattern. The gain and the directivity of the split octagonal ring antenna are shown in Fig. 11 and Fig. 12, respectively. The gain is greater than one dBi in all active bands, and the directivity is greater than two dBi in all operating bands. Fig. 13 is a comparison plot showing the measured return loss versus the simulates return loss. Table 2 shows the comparison of the proposed antenna with the literature.

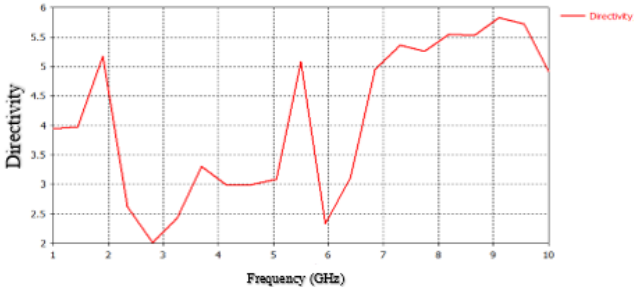

Fig. 12. Metamaterial ring antenna – directivity vs. frequency.

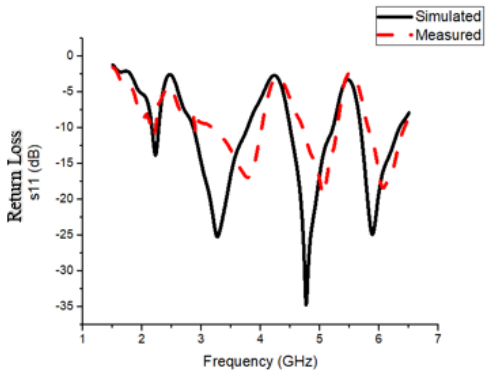

Fig. 13. Simulated vs. measured S11 plot.

Table 2. Comparison of the proposed antenna with the literature.

Procedure used	L × W [mm]	Centre frequency [GHz]
Hexagonal patch, fractal	75 × 75	1.575, 5.9, 7.2
Triangular patch, slot	30 × 28	1.6, 2.8, 5.7, 9.6
Crescent shape patch	31 × 35	11.30, 18.07, 20.72
Fractal, L shape slot and SRR	30 × 24.8	3.3, 5.5, 7.3, 9.9
ELC	35 × 35	3.77, 5.4
Metamaterial, Stub (Proposed antenna)	26 × 21	2.23, 3.28, 4.77, and 5.89

5. CONCLUSION

The stub-based antenna under consideration was specifically developed for quad-band satellite communication applications. It offers adaptability for ISM, WLAN, WiMAX and 5G sub-6 GHz operation. The device operates at frequencies of 2.23 GHz, 3.28 GHz, 4.77 GHz and 5.89 GHz, and achieves multiband capability by using stubs, which has been confirmed by analysis of simulated surface current distribution. A parametric analysis is used to determine the most effective values for important factors such as the position of the stub, the length of the ground and the width of the ring. This study helps to ensure that the performance is efficient. The study confirms the role of stubs in facilitating multiband operations. The simulated and measured results for S11, gain, E-plane and H-plane patterns agree and confirm the performance of the antenna. This antenna provides a strong and versatile solution for various wireless applications due to its simple design, small size, high gain, impedance matching and uniform radiation pattern.

REFERENCES

[1] Mood, Y., Pandeeswari, R. (2023). A novel SRR metamaterial inspired CPW-fed dual band MIMO antenna for Sub-6 GHz 5G application. *Wireless Personal Communications*, 130 (2), 1277-1293. https://doi.org/10.1007/s11277-023-10331-5

[2] Zhang, X., Chen, Z., Ye, X. (2024). A W-Band high-gain low-sidelobe circular-shaped monopulse antenna array based on dielectric loaded waveguide. *IEEE Access*, 12, 64997-65006. https://doi.org/10.1109/ACCESS.2024.3397304

[3] Datta, R., Shaw, T., Mitra, D. (2017). Miniaturization of microstrip Yagi array antenna using metamaterial. *Progress in Electromagnetics Research C*, 72, 151-158. http://dx.doi.org/10.2528/PIERC16122102

[4] Selvi, N. T., Pandeeswari, R., Selvan, P. N. T. (2018). An inset-fed rectangular microstrip patch antenna with multiple split ring resonator loading for WLAN and RF-ID applications. *Progress in Electromagnetics Research C*, 81, 41-52. http://dx.doi.org/10.2528/PIERC17110102

[5] Pandeeswari, R. (2018). Complimentary split ring resonator inspired meandered CPW-fed monopole antenna for multiband operation. *Progress in Electromagnetics Research C*, 80, 13-20. http://dx.doi.org/10.2528/PIERC17101402

[6] Dong, Y., Itoh, T. (2012). Metamaterial-based antennas. *Proceedings of the IEEE*, 100 (7), 2271-2285. https://doi.org/10.1109/JPROC.2012.2187631

[7] Nejdi, I. H., Bri, S., Marzouk, M., Ahmad, S., Rhazi, Y., Ait Lafkih, M., Ghaffar, A., Hussein, M. (2023). UWB circular fractal antenna with high gain for telecommunication applications. *Sensors*, 23 (8), 4172. https://doi.org/10.3390/s23084172

[8] Vallappil, A. K., Rahim, M. K. A., Khawaja, B. A., Iqbal, M. N. (2024). A miniaturized metamaterial-loaded switched-beam antenna array system with enhanced bandwidth for 5G applications. *IEEE Access*, 12, 6684-6697. https://doi.org/10.1109/ACCESS.2024.3351475

[9] Sam, P. J. C., Gunavathi, N. (2020). A tri-band monopole antenna loaded with circular electric–inductive–capacitive metamaterial resonator for wireless application. *Applied Physics A*, 126, 774. https://doi.org/doi:10.1007/s00339-020-03952-1

[10] Lakshmi, M. L. S. N. S., Prasad Jones Christydass, S., Kannadhasan, S., Anguraj, K., Chatterjee, J. M. (2023). Polarization stable triband thin square-shaped metamaterial absorber. *International Journal of Antennas and Propagation*. https://doi.org/10.1155/2023/6065300

[11] Kaur, K., Kumar, A., Sharma, N. (2023). A novel design of ultra-wideband CPW-fed printed monopole antenna for Wi-MAX, WLAN and X-band rejection characteristics. *Analog Integrated Circuits and Signal Processing*, 114 (1), 143-157. https://doi.org/10.1007/s10470-022-02132-w

Received January 19, 2024
Accepted July 22, 2024